Journal of Catalysis 263 (2009) 34–41

Contents lists available at ScienceDirect

Journal of Catalysis

www.elsevier.com/locate/jcat

Identification of reaction intermediates during hydrogenation of CD_3CN on Raney-Co

Peter Schärringer, Thomas E. Müller [*], Andreas Jentys, Johannes A. Lercher

Lehrstuhl 2 für Technische Chemie, Department Chemie, Technische Universität München, Lichtenbergstraße 4, 85747 Garching, Germany

ARTICLE INFO

Article history:
Received 13 July 2008
Revised 15 January 2009
Accepted 20 January 2009
Available online 14 February 2009

Keywords:
Hydrogenation
Nitrile
Amine
Raney-Co
Inelastic neutron scattering
INS
Surface intermediates
Nitrene
Kinetics
Selectivity
H/D exchange
Heat of adsorption

ABSTRACT

Reaction intermediates formed on the surface of Raney-Co after co-adsorption of acetonitrile-*d*$_3$ (CD_3CN) and hydrogen were investigated by inelastic neutron scattering (INS). Detailed information on the structure of the adsorbed molecules was obtained by comparison of the spectra of potential reaction intermediates with reference spectra of H_2, CD_3CN, and $CD_3CH_2NH_2$ as well as INS spectra calculated by *ab initio* methods. We concluded that CD_3CN reacted preferentially with hydrogen bound to η^3 sites on the Co-001 plane. On the surface, a mixture of a nitrene-like intermediate and co-adsorbed $CD_3CH_2NH_2$ was formed, as indicated by a strong CH_2 twisting vibrational mode, which decreased in intensity relative to the other CH_2 vibrational modes, when the amount of hydrogen was increased. The surface study is complemented with detailed catalyst characterisation as well as kinetic data on the hydrogenation of acetonitrile-*d*$_3$.

1. Introduction

Primary amines are feedstock in the production of many chemicals as, e.g., fibres for textiles and surface-active compounds. One important industrial process for their production is the hydrogenation of the corresponding nitriles over transition metal catalysts [1], which is usually accompanied by the formation of secondary and tertiary amines [2]. In certain applications even trace amounts of the by-products have to be avoided [3,4]. For the hydrogenation of nitriles, skeletal Raney catalysts based on Co or Ni are widely used [5]. Compared to other transition metals, Co exhibits the highest selectivity to primary amines, but provides relatively low activity [6]. Structure–selectivity correlations have been established recently for Raney-Co [7–9]; however, for further optimization of the catalysts with respect to selectivity, understanding the mechanism of by-product formation appears essential.

Already in 1923, von Braun suggested that the side reactions proceed *via* reactive aldimine intermediates [2] and ever since numerous mechanistic discussions were based on this proposal [10–12]. As direct evidence for the aldimine has not been reported [13], other possible surface intermediates, such as carbenes and nitrenes, were considered in the discussion [13–16]. For studying the sorption of organic molecules on metal surfaces, inelastic neutron scattering (INS) has proven a useful tool [17–21]. INS is particularly sensitive for vibrations involving hydrogen atoms, as the scattering cross-section of hydrogen is 10–100 times larger than that of all other elements [22]. Therefore, INS is a valuable technique to study the sorption of hydrogen and nitriles on Raney catalysts [7,23–25].

To unravel the elementary steps of nitrile hydrogenation on Raney-Co, catalysts and reaction profiles were explored in detail, with special emphasis on the identification of surface intermediates. As model system, the co-adsorption of acetonitrile-*d*$_3$ (CD_3CN) and hydrogen was investigated. The use of acetonitrile-*d*$_3$ enabled us to detect surface reactions associated with the nitrile group, while keeping the scattering contributions of the methyl group low. Thus, an improved differentiation between the reactant and hydrogenated surface intermediates could be obtained. The goal was to identify the C–H and N–H vibrations of partially hydrogenated surface intermediates during the hydrogenation of the CN triple bond. Understanding of the vibrational features was accomplished by simulating the INS spectra.

---

[*] Corresponding author. Current address: CAT Catalytic Center, ITMC, RWTH Aachen University, Worringerweg 1, 52074 Aachen, Germany. Fax: +49 241 8028593.
E-mail address: thomas.mueller@catalyticcenter.rwth-aachen.de (T.E. Müller).

0021-9517/$ – see front matter © 2009 Elsevier Inc. All rights reserved.
doi:10.1016/j.jcat.2009.01.009

2. Experimental

2.1. Materials

Raney-Co 2700 (1.85 wt% Al; 97.51 wt% Co; 0.3 wt% Fe and 0.34 wt% Ni, Grace Davison division of W.R. Grace and Co.) was received as aqueous suspension. It was washed with de-ionized water under nitrogen atmosphere until the pH of the washing water was seven. Due to its sensitivity to oxygen, the catalyst was stored and handled under inert atmospheres throughout all further steps. The remaining water was removed by drying in vacuum ($p < 1$ kPa) for 30 h at 323 K. CD_3CN (Deutero GmbH), CH_3CN (Fluka) and acetaldehyde (Riedel–de Haën) with a purity of 99.5% each were used as received. Ethylamine-d_3 ($CD_3CH_2NH_2$) was obtained by hydrogenation of CD_3CN over Raney-Co 2700.

2.2. Catalyst characterization

2.2.1. H_2 chemisorption and N_2 physisorption

H_2 chemisorption and N_2 physisorption (BET) measurements were performed on a Sorptomatic 1990 instrument (ThermoFinnigan). For both measurements, the catalyst sample (∼1 g) was outgassed for 6 h at 473 K ($p < 1$ mPa). The BET measurement was conducted at 77 K. H_2 chemisorption was carried out at 308 K with an equilibrating time of 2–180 min for each pressure step. Equilibration was continued until the pressure deviation was <0.27 mbar within a 2-min period. Isotherms were measured twice on each sample. Between the two measurements, the sample was evacuated to 10^{-3} mbar for 1 h. The second isotherm (physisorbed H_2) was subtracted from the first isotherm (chemisorbed and physisorbed hydrogen). The amount of hydrogen adsorbed was determined by extrapolating the linear part of the difference isotherm ($p > 6.5$ kPa) to zero pressure.

2.2.2. Adsorption of CD_3CN followed by thermogravimetry and calorimetry

The adsorption of gaseous CD_3CN on Raney-Co was investigated on a Setaram TG-DSC 111 thermoanalyzer. After outgassing the catalyst sample (∼24 mg) for 6 h at 473 K ($p < 0.1$ mPa), CD_3CN was adsorbed at 308 K using pressure pulses of 0.02–2.5 mbar up to ∼11 mbar. The weight increase and the corresponding heat flux were recorded for each pulse. The sorption isotherm was fitted with a dual-site Langmuir model:

$$q = \sum_{j=1}^{n} q_j^{\mathrm{sat}} \frac{K_j \cdot p^*}{1 + K_j \cdot p^*}, \tag{1}$$

where K_j is the equilibrium constant for sorption on site j, q_j^{sat} denotes the maximum sorption capacity on site j (molecules/metal atom), and p^* is the partial pressure of CD_3CN normalized to standard conditions ($p^* = p/p^0$).

2.3. Hydrogenation experiment

The hydrogenation of CD_3CN was conducted in a semi-batch mode at constant hydrogen pressure. Raney-Co (1 g) was suspended under inert atmosphere in the reaction mixture composed of CD_3CN (40 cm^3) and hexane (40 cm^3). Hexane was used as solvent and internal standard for GC chromatography. An autoclave (160 cm^3; Parr Instrument) was charged with the suspension under a flow of nitrogen. After closing, the reactor was purged with nitrogen to remove oxygen. The reaction mixture was heated to the reaction temperature (383 K), the reactor pressurized rapidly with hydrogen to 45 bar and the reaction started by starting the stirrer (1500 rpm). Samples for GC and NMR analysis were withdrawn periodically through a dip-tube with a filter for solids. GC analysis was carried out on an HP Gas Chromatograph 5890 equipped with a cross linked 5% diphenyl-95% dimethylpolysiloxane column (Rtx-5 Amine, 30 m, Restek GmbH). ^{1}H NMR and ^{2}H NMR measurements were carried out on a Bruker DPX-400 instrument (400 MHz) with CD_3Cl as solvent containing 1 vol% trimethylsilane as standard. An assignment of the signals is given in Table 1. The selectivity was calculated as the ratio of the product to the amount of CD_3CN converted.

Table 1
Assignment of the chemical shift in the NMR-spectra of the product mixture of CD_3CN hydrogenation [26,27]. Note that the ^{1}H and ^{2}D chemical shifts are identical.

Molecule		Chemical shift[a] (ppm)	Assignment
n-Hexane	A	1.27	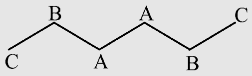
	B	1.27	
	C	0.88t	
Acetonitrile	A	1.98	
Ethylamine	A	2.74	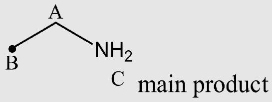
	B	1.10t	
	C	(0.5–4.0)*	
Di-ethylamine	A	1.10	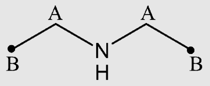
	B	2.64	
N-Ethylidene-ethylamine	A	3.35	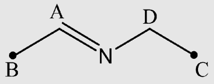
	B	1.80	
	C	1.20	
	D	Not observed	

[a] t—triplet, •—CD_3, ∗—position variable.

2.4. Inelastic neutron scattering experiments

Samples of pre-dried Raney-Co (each ∼45 g) were transferred under inert atmosphere to cylindrical aluminium containers with 7.5 cm height and 2.3 cm diameter. The samples were activated in vacuum ($p < 1$ mPa) at 473 K for 6 h. Subsequently, CD_3CN was added as liquid (Table 2). The amount of CD_3CN was calculated with respect to two boundary conditions. To obtain sufficient signal intensity, it was necessary to use a relatively high amount of CD_3CN. On the other hand, free CD_3CN in the sample container had to be avoided to assure that only CD_3CN or reaction intermediates, which were adsorbed on the catalyst, contribute to the signal. Consequently, a ratio of 0.30 $\mathrm{mol}_{CD_3CN}\,(\mathrm{Co}_{\mathrm{Surface}})^{-1}$ was chosen. For adsorption of ethylamine-d_3 ($CD_3CH_2NH_2$), the same molar loading was used. Four sample containers were charged with CD_3CN. Three of those were equilibrated with hydrogen in a ratio of 0.5, 1.5, and 2.0 $\mathrm{mol}_{H_2}\,(\mathrm{mol}_{CD_3CN})^{-1}$ (see Table 2). After sealing, the aluminium containers were heated to 333 K for 10 h to ensure even distribution of the adsorbate and to initiate the reaction of CD_3CN with hydrogen.

Inelastic neutron scattering measurements (INS) were performed on the 3-axis spectrometer IN1 at the Institut Laue-Langevin (Grenoble, France) using a Beryllium filter-analyser (BeF), a Cu (220) monochromator and neutrons from the hot source [28]. For the INS experiments, the sample containers were inserted in the cryostat and cooled to 10 K. The spectra were recorded with a resolution of 16, 8 and 32 cm^{-1} in the energy ranges 213–760, 760–1745 and 1745–2070 cm^{-1}, respectively. In order to test the reproducibility of sample preparation and INS measurements, the same experiments were carried out in two different mea-

Table 2
Amounts of catalyst, CD_3CN, $CD_3CH_2NH_2$ and hydrogen charged into the sample cells for INS measurement.

Sample	Amount of catalyst (g)	Amount of CD_3CN or $CD_3CH_2NH_2$ (mmol)	Amount of hydrogen (mmol)	Molar ratio H_2/CD_3CN
Raney-Co	45.42	–	–	–
Raney-Co + H_2	38.94	–	10.36	–
Raney-Co + CD_3CN	44.98	8.80	–	–
Raney-Co + CD_3CN + 0.5 eq. H_2	45.23	8.85	4.43	0.5
Raney-Co + CD_3CN + 1.5 eq. H_2	45.27	8.86	13.29	1.5
Raney-Co + CD_3CN + 2.0 eq. H_2	44.70	8.75	17.50	2.0
Raney-Co + $CD_3CH_2NH_2$	45.80	8.96	–	–

surement cycles. The results from the two cycles showed good agreement.

2.5. Computational methods

The vibrational frequencies of the characteristic groups in the INS spectra were calculated after optimizing the structure of the different molecules with respect to the total energy using density functional theory (DFT) as implemented in GAUSSIAN 03 [29]. The B3LYP hybrid functional and a 6-31G** basis set were applied. The displacement vectors calculated for each vibrational mode were used to derive the INS-spectra with the program a-CLIMAX [30,31] using spectral peak width of 15 cm^{-1}. The vibrational modes were visualized and assigned with Molview 3.0.

3. Results

3.1. Adsorption of H_2 and CD_3CN on Raney-Co

Although Raney-Co consists almost entirely of metallic cobalt [32], the surface is structured heterogeneously containing different adsorption sites. In H_2 chemisorption measurements, both irreversibly (chemisorbed) and reversibly (physisorbed) bound hydrogen was observed (Fig. 1). Assuming a stoichiometry of 1 H atom per Co atom for chemisorption, the number of surface metal atoms was calculated to 0.36 $mmol\,g_{Cat}^{-1}$. Considering also the weakly adsorbed hydrogen and assuming a stoichiometry of 2 H atoms per Co atom for physisorption, the overall number of surface metal atoms adsorbing H_2 was determined to 0.46 $mmol\,g_{Cat}^{-1}$. Assuming a transversal section of 6.5 Å^2 for Co, the metal surface area was calculated to 18.7 $m^2\,g_{Cat}^{-1}$, which is comparable to a BET area measured by N_2 physisorption of 29.1 $m^2\,g_{Cat}^{-1}$.

Insight into the relative number and strength of the sorption sites was obtained by adsorption of CD_3CN. The sorption isotherm (Fig. 2) can be well described by a dual-site Langmuir model [33]. The shape of the isotherm indicates that the equilibrium constant and, thus, the heat of adsorption for the first sorption process must be much higher than for the second sorption process. This was confirmed by measuring the differential heat of adsorption (Fig. 3), which was high at low uptake (200–215 $kJ\,mol^{-1}$ at <0.08 $molecules\,(Co_{Surface})^{-1}$) and showed a sharp decrease to an almost constant value of 57–65 $kJ\,mol^{-1}$ at higher coverage (Table 3). The remarkably high heat of adsorption at low coverage can be attributed to chemisorption of CD_3CN on sites, which strongly interact with the sorbate. Most likely, chemisorption involves a surface reaction (*vide infra*). Note that heat of chemisorption is higher than the heat of full hydrogenation of CD_3CN ($\Delta H_R = 120$ $kJ\,mol^{-1}$). Comparison with the hydrogen chemisorp-

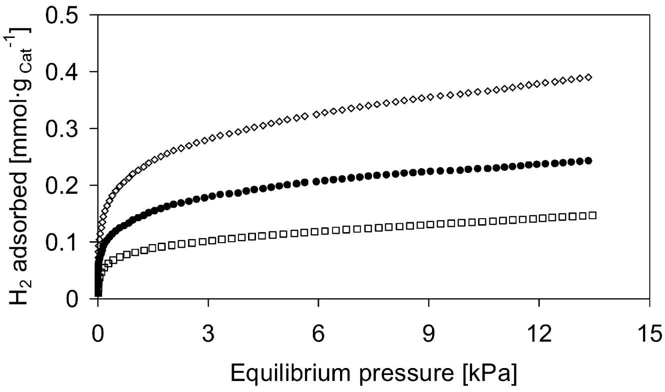

Fig. 1. H_2 chemisorption isotherm for Raney-Co at $T = 308$ K. (◇) After outgassing for 6 h at $T = 473$ K, (□) after subsequent evacuation at $T = 308$ K ($p < 1$ mPa for 1 h), (●) difference of (◇) and (□).

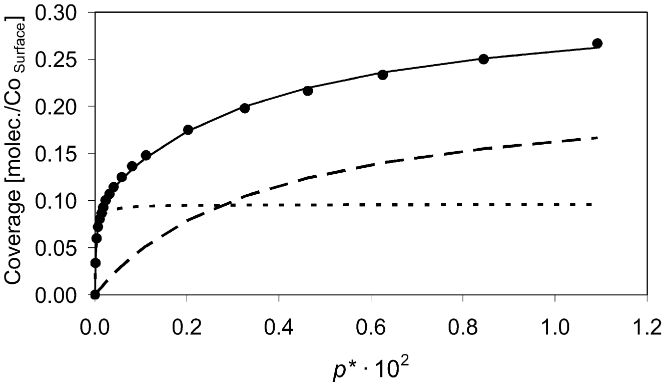

Fig. 2. Sorption isotherm for CD_3CN on Raney-Co at 308 K and contribution of the individual sorption processes according to a dual-site Langmuir model. (●) Experimental data, (···) calculated isotherm for sorption process 1 with K_1 and q_1^{sat}, (– – –) calculated isotherm for sorption process 2 with K_2 and q_2^{sat}, (—) sum of both isotherms. p^* is the partial pressure of CD_3CN normalized to standard conditions ($p^* = p/p^0$).

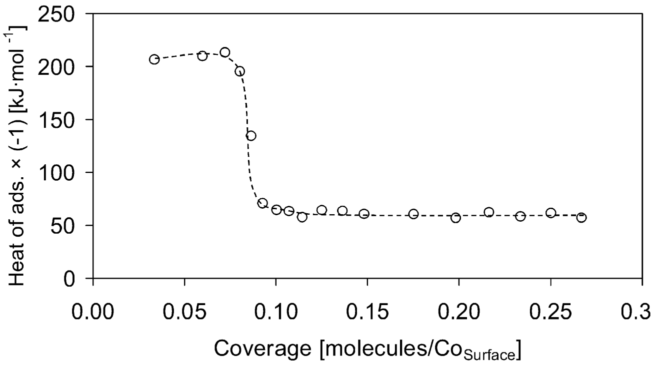

Fig. 3. Differential heat of adsorption of CD_3CN on Raney-Co from calorimetry at 308 K.

Table 3
Data for the adsorption of CD_3CN on Raney-Co obtained from fitting the experimental sorption isotherm with a dual site Langmuir model and direct measurement of the differential heat of adsorption.

Sorption process	q_j^{sat} $(molec.\,(Co_{Surface})^{-1})$	K_j	$\Delta H_{ads} \times (-1)$ $(kJ\,mol^{-1})$
1	9.62×10^{-2}	3.94×10^4	208 ± 8
2	$>22.2 \times 10^{-2}$	2.73×10^2	61 ± 4

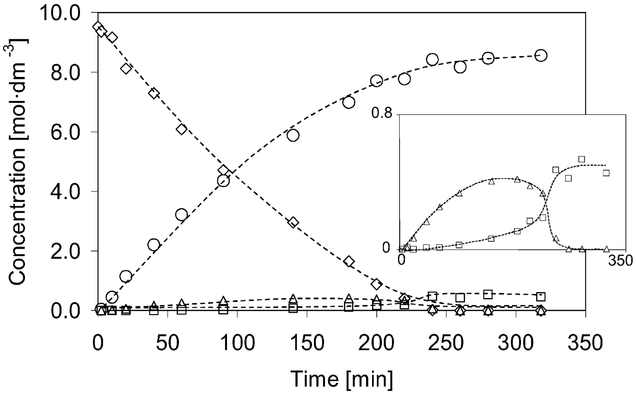

Fig. 4. Concentration profile for the hydrogenation of CD_3CN over Raney-Co at 383 K, $p = 45$ bar and $c_0(CD_3CN) = 9.52$ mol dm^{-3}. (◇) CD_3CN, (○) ethylamine, (△) *N*-ethylidene-ethylamine, (□) di-ethylamine.

tion data indicates that an overlayer is formed, whereby at a coverage of 0.08 molecules $(Co_{Surface})^{-1}$ one surface intermediate occupies twelve Co surface atoms. An alternative explanation is that all reactive hydrogen on the surface had been consumed. At higher coverage, CD_3CN is adsorbed either without associated surface reaction, on sites with weaker interaction with CD_3CN, or restructuring of the overlayer consumes energy.

3.2. *H/D exchange and selectivity in the hydrogenation of CD_3CN*

Motions involving H atoms exhibit particularly high signal intensity in INS and we expected to be able to identify H atoms in partially hydrogenated surface species. The reaction of CD_3CN and H_2 over Raney-Co was studied. As we had to exclude that exchange of H atoms with the CD_3 group occurs, hydrogenation of CD_3CN in the liquid phase was analysed first. A typical concentration profile of the reaction is shown in Fig. 4. The main product of the hydrogenation reaction was ethylamine, which was formed with a selectivity of ~90%. Ethylamine and small amounts of *N*-ethylidene-ethylamine were observed as primary products. Only after most of CD_3CN (~90%) had been converted, the *N*-ethylidene-ethylamine intermediate was hydrogenated to the secondary product di-ethylamine.

^1H NMR and ^2H NMR spectra of the final product mixture are shown in Fig. 5 (for assignment of the signals, see Table 1). The main product was $CD_3CH_2NH_2$ (signals at 1.10, 1.02 and 2.74 ppm in ^2H, ^1H and ^1H NMR, respectively). Peaks with low intensity at 2.63 and 2.74 ppm in ^2H NMR correspond to $(CD_3CH\mathit{D})_2NH$ and $CD_3CH\mathit{D}NH_2$, respectively. Integration of the signals showed that only 0.83% of the deuterium atoms were found in other positions than the CD_3-group. Thus, only little H/D exchange occurred at 383 K, which is essential for interpretation of the INS measurements (*vide infra*). Note, that the low degree of H/D exchange also indicates that the equilibrium between an imine (suggested as intermediate in literature, see e.g., [17]) and the corresponding enamine is of no consequence for interpretation of the INS data in this study.

3.3. *Results of INS measurements*

3.3.1. *Hydrogen adsorption on Raney-Co studied by INS*

To evaluate the preferred adsorption mode of hydrogen, INS spectra of hydrogen adsorbed on Raney-Co were recorded in comparison to the parent catalyst (Fig. 6). In both spectra, scattering contributions of hydrogen gave rise to a broad peak between 600 and 1100 cm^{-1}, which was centred at around 850 to 900 cm^{-1}. For the parent Raney-Co, this indicates that some hydrogen could not be removed during outgassing in high vacuum. The strongly bound hydrogen can be attributed to hydrogen adsorbed on η^3 sites (Table 4). Admission of hydrogen led to an increase in the scattering contributions over the entire spectral range. A distinct peak at 504 cm^{-1} can be assigned to hydrogen adsorbed on η^3 sites with C_{3v} symmetry in the 001 plane. Small scattering contributions above 1500 cm^{-1} are probably an overtone of the strong feature at 800 cm^{-1} or due to some hydrogen adsorbed on σ sites. However, the signal intensity was small compared to multiple-bound hydrogen.

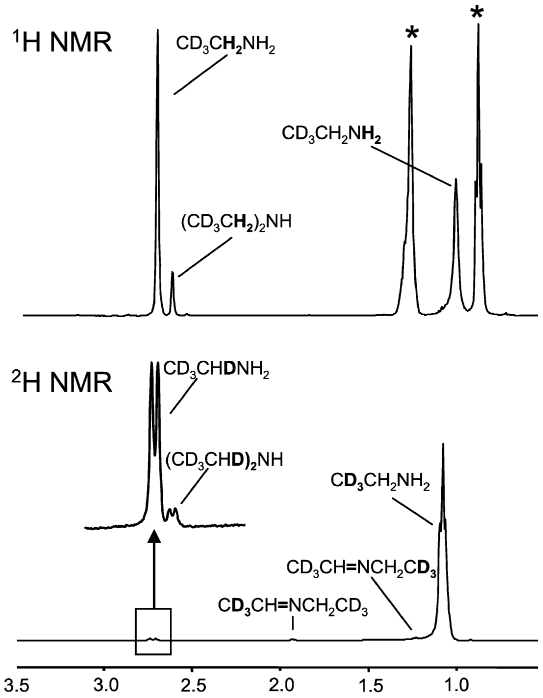

Fig. 5. NMR spectra of the product mixture of the hydrogenation of CD_3CN. *—hexane.

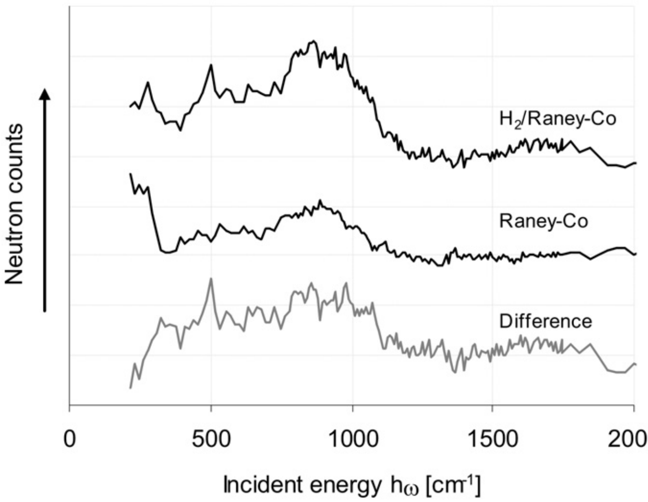

Fig. 6. INS spectrum of hydrogen adsorbed on Raney-Co in comparison to the parent Raney-Co, which was activated by outgassing in high vacuum. The background determined by measurement of an empty sample container is subtracted from each of the two spectra.

3.3.2. *Adsorption of acetonitrile on Raney-Co and formation of surface intermediates*

After adsorption of CD_3CN on Raney-Co, the INS spectrum (for comparison included in Fig. 8) exhibited a distinct peak at

Table 4
Vibrational frequencies and assignment of sorption sites for hydrogen adsorbed on Raney-Co. The assignment of the hydrogen vibrations follow the detailed DFT analysis reported previously [7].

ν_{INS}[a]	ν_{INS}[b]	ν_{INS}[c]	Coord. mode	Plane	Symmetry	Vibration[c,d,e]
278	278	250	η^4	101	D_{4h}	Co_4–H sym stretch
536	504	573	η^3	001	C_{3v}	Co_3–H antisym stretch
632	648	637	η^3	101	C_{3v}	Co_3–H antisym stretch
777	777	782	η^3	101	C_{3v}	Co_2–H asym stretch
890	866	894	η^3	001	C_{3v}	Co_2–H antisym stretch
1020	1020	1100	η^3	001	C_{3v}	Co_3–H sym stretch
–	>1600	1660	σ	–	–	Co–H stretch[f]

[a] This work (activated Raney-Co).
[b] This work (activated Raney-Co after addition of hydrogen).
[c] Ref. [7].
[d] Ref. [25].
[e] Ref. [23].
[f] Probably hydrogen on 1-fold sites. DFT calculations of single bound hydrogen on 101 and 001 planes indicate a peak position at 1800–1860 cm^{-1}.

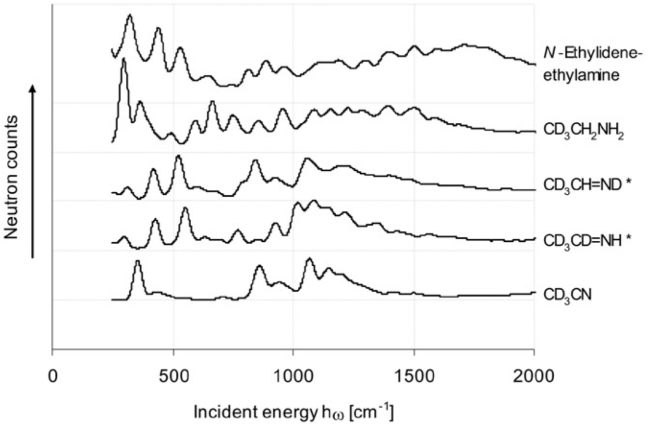

Fig. 7. Gas phase INS spectra calculated for the reactant CD_3CN, possible intermediates, and product $CD_3CH_2NH_2$. *N*-Ethylidene-ethylamine is partially deuterated $CD_3CH=NCH_2CD_3$. To differentiate between CH and NH vibrational modes, H and D were exchanged for imines (marked with *) calculated as model for surface imine species. The spectra were calculated at resolution 15 cm^{-1}.

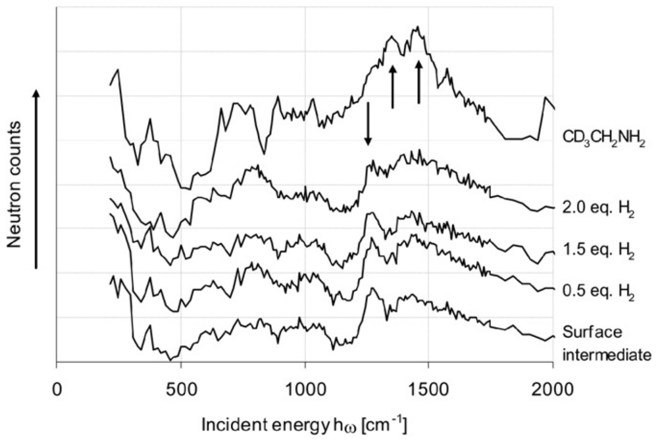

Fig. 8. INS spectra of hydrogen co-adsorbed with CD_3CN on activated Raney-Co. The amount of hydrogen was varied in the range H_2/CD_3CN 0, 0.5, 1.5, and 2.0. The CD_3CN loading was 0.18 molecules per surface metal atom. For comparison, the spectrum of $CD_3CH_2NH_2$ adsorbed on activated Raney-Co is also given. The spectrum of activated Raney-Co has been subtracted from all spectra shown.

Table 5
Comparison of the vibrational frequencies of gas phase CH_3CN and CD_3CN.

CH_3CN		CD_3CN		Assignment
IR gas[a]	INS[b]	IR[c]	DFT[d]	
	75			Lattice mode
	120			Lattice mode
	160			Methyl torsion
361	396	347	354	CCN bend
920	928	902	842	CC stretch
1041	1056	(833)	(875)	$CH_3/(CD_3)$ rock
1389	1390	(1093)	(1138)	$CH_3/(CD_3)$ sym bend
1454	1453		(1067)	$CH_3/(CD_3)$ antisym def
2268		2291	2198	CN stretch
2954		(2110)	(2268)	$CH_3/(CD_3)$ sym stretch

[a] Ref. [37].
[b] Ref. [24].
[c] Ref. [34]. Calculated from data on CH_3CN; for shift ratios, see the reference.
[d] This work.

Table 6
Selected literature data on the vibrations of CD_3CN and CH_3CN adsorbed on various metals.

CH_3CN			CD_3CN	Assignment
Raney-Ni[a]	Ni(111)[b]	Pt(111)[c]	Pt(111)[c]	
52				CH_3 torsion
100				Hindered translations and motions
160				CH_3 torsion
		280	265	Pt–MeCN stretch sym
		410	385	Pt–MeCN stretch asym
385, 392	360			CCN bend
520	520	605	580	CCN bend
	900 (sh)	950	930	CC stretch
1047, 1042	1020	1060	(850)	$CH_3/(CD_3)$ rock
1427, 1450	1400	1375	(1100)	$CH_3/(CD_3)$ sym bend
		1435		CH_3 deg bend
	1680	1615	1625	CN stretch
	2910			CH_3 sym stretch

[a] Ref. [24].
[b] Refs. [34,35].
[c] Ref. [36].

375 cm^{-1}, a broad scattering region with strongly overlapping features between 600 and 1100 cm^{-1}, a distinct peak at 1278 cm^{-1} and a broad peak starting at 1300 cm^{-1} with a long tailing to 1800 cm^{-1}. The experimental spectrum differs significantly from the spectrum for CD_3CN in the gas phase, for which bands at 354, 842, 875, 1067, 1138, 2198 and 2268 cm^{-1} were calculated (Fig. 7). The positions of the calculated vibrational modes agree well with reference data on CH_3CN (Table 5). The peaks with highest intensity were assigned to the C–C–N bending mode at 354 cm^{-1}, the C–C stretching mode at 842 cm^{-1} and the CH_3 symmetric bending mode at 1138 cm^{-1}. The difference between experiment and simulation is striking and in contrast to reports on CH_3CN and CD_3CN adsorbed on other late transition metals (Table 6). Upon adsorption of CD_3CN on Pt(111) or CH_3CN on Ni(111), only few selected vibrational modes were influenced, while the general features of the spectra remained the same [27,34,36]. The contrasting change upon adsorption of CD_3CN on Raney-Co observed here strongly suggests that a new compound was formed.

3.3.3. *Adsorption of ethylamine on Raney-Co*

To identify the surface species formed by reaction of CD_3CN with residual hydrogen, the spectra were compared to those of $CD_3CH_2NH_2$ adsorbed on Raney-Co (Fig. 8). Assignment of the bands was based on DFT calculations for $CD_3CH_2NH_2$ in the *trans* form, as it was suggested that it occurs more frequently on metal surfaces compared to the *gauche* form [40]. Note that $CD_3CH_2NH_2$ is adsorbed preferentially through its nitrogen lone pair electrons [38,40]. As for CD_3CN (Table 5), there are small differences in the vibrational modes of CH_2, NH_2, CCN, CC, and CN between the INS signal positions calculated and the experimental IR bands for $CH_3CH_2NH_2$ in the gas phase [39,41] and ethylamine adsorbed on Ni(111) [40] (Table 7). The remarkable difference in the CH_3

Table 7
Vibrational frequencies of $CH_3CH_2NH_2$ and $CD_3CH_2NH_2$ in the gas phase and adsorbed on different metals.

Gas phase			Ni(111)[c] HREELS	Raney-Co[b] INS	Assignment
Gauche[a]	Trans[a]	DFT[b]			
		297		245	NH_2 rock
403		362		375	CCN bend
		664		664	CH_2 rock
		755		745	CD_3/bend
773	790	850	760	891	NH_2 wag
892	882	975	880	1036	CC stretch
1016		955			NH_2 twist
1016	1119	(1086)	1140	(1100)	CH_3/(CD_3) d rock
1086	1055	1122	1080	1132	CN stretch
1238	1350	1226		1293	CH_2 twist
1378					CH_3 sym def
1397		1387	>1360	1359	CH_2 wag
1465			>1440		CH_3 d def
1487		1508		1455	CH_2 scission
1622		1673	1540	1575	NH_2 scission
2880		(2176)	2960	–	CH_3/(CD_3) sym stretch
		(2296)		–	CH_3/(CD_3) asym stretch
2885		3040	2680	–	CH_2 sym stretch

[a] Refs. [39–41], $CH_3CH_2NH_2$.
[b] This work, $CD_3CH_2NH_2$ in the *trans* form.
[c] Ref. [35].

symmetric stretch band (shift from 2880 to 2176 cm^{-1}) is due to the exchange of H by D. The band at 1293 cm^{-1} in the experimental spectrum of $CD_3CH_2NH_2$ was assigned to CH_2 twisting. For this band, DFT calculations predict a position at 1226 cm^{-1}, which is probably due to changes during adsorption on Raney-Co. Conversely, the CH_2 wagging mode was shifted to lower frequency. The other band positions in INS were similar to gas phase, DFT calculations, and literature data for adsorbed ethylamine and, thus, could be assigned accordingly. The shoulder at 407 cm^{-1} was also observed in the DFT results (Fig. 7), but could not be assigned. An additional peak at 455 cm^{-1} may be due to cobalt–nitrogen vibrations, as its position is comparable to nickel–nitrogen vibrations observed at 500 cm^{-1} for ethylamine on Ni(111) [40] and at 490 cm^{-1} for NH_3 on Ni(111) [43]. DFT simulation showed bands at 499 and 596 cm^{-1} (not assigned), which were either overlapped or too low in intensity to identify them in the experimental INS data. A band at 1293 cm^{-1} (shoulder) observed experimentally may be attributed to a shifted CH_2 twist, found at 1226 cm^{-1} in the simulated vibrations. In general, the relative peak intensity in the experiment is comparable to that of DFT calculations in the lower frequency region (up to $\sim$1200 cm^{-1}). At higher incident energy, the intensity of the bands is high compared to the simulation.

3.3.4. Co-adsorption of CD_3CN and hydrogen on Raney-Co

To explore the structure of partially hydrogenated species, a series of INS spectra of adsorbed CD_3CN was measured in the presence of increasing amounts of hydrogen (Fig. 8). All spectra showed characteristic features similar to those observed, when CD_3CN was adsorbed on Raney-Co. With increasing amount of hydrogen, the scattering characteristics changed in such way that the spectra became more similar to the reference spectrum of $CD_3CH_2NH_2$.

For the four samples, where CD_3CN was adsorbed on activated Raney-Co with varying amounts of hydrogen (H_2/CD_3CN 0, 0.5, 1.5, and 2.0) a band at 262 cm^{-1} was observed. Note that during adsorption of CD_3CN on activated Raney-Co (H_2/CD_3CN 0) a surface intermediate was formed. The band at 262 cm^{-1} is assigned to hydrogen co-adsorbed on η^4 sites with D_{4h} symmetry. The CCN bending mode was located at 375 cm^{-1}. A band at 407 cm^{-1} was observed, but could not be clearly identified. A weak band at 504 cm^{-1} was assigned to Co_3–H anti-symmetric stretch on η^3 coordination modes. In the region between 600 cm^{-1} and 1200 cm^{-1} features of the partially hydrogenated or product molecules were overlapping with scattering contributions of co-adsorbed hydrogen making unambiguous peak assignment difficult. However, it can be stated that with increasing amount of hydrogen a broad band centred at 777 cm^{-1}, which was previously assigned to Co_2–H asymmetric stretch η^3 sites, increased in intensity. The band at 745 cm^{-1} may be due to CD_3 bending modes. NH_2 wag and CC stretch modes found at 891 cm^{-1} and 1036 cm^{-1} for $CD_3CH_2NH_2$, respectively, were either relatively weak or overlapped by hydrogen vibration modes as no distinct peaks were found in that region. With exception of the hydrogen band at 777 cm^{-1}, no clear trend in the intensity of the bands was obtained up to 1200 cm^{-1}. An interesting band was observed at 1278 cm^{-1} exhibiting high intensity for the sample where only CD_3CN had been adsorbed. Compared to the broad signal above 1300 cm^{-1} the relative intensity of this band decreased with increasing amount of hydrogen. Note that in the case of $CD_3CH_2NH_2$, a shoulder at 1293 cm^{-1} was attributed to a CH_2 twisting mode.

For all samples with CD_3CN and CD_3CN co-adsorbed with hydrogen, a broad band between 1300 and 1800 cm^{-1} similar to the pattern observed for $CD_3CH_2NH_2$ was found. Compared to the band at 1278 cm^{-1}, the relative intensity of the band increased with increasing amount of hydrogen. This is an indication that upon addition of hydrogen the intermediate species was converted resulting in an increasing amount of $CD_3CH_2NH_2$. However, the distinct peaks as found for $CD_3CH_2NH_2$ at 1359, 1455, and 1575 cm^{-1} were not as well resolved suggesting that other molecules were also present, which exhibit a different scattering behaviour. It is concluded that the broad band between 1300 and 1800 cm^{-1} was a result of overlapping signals of $CD_3CH_2NH_2$ and the intermediate species.

4. Discussion

4.1. Role of hydrogen sorption strength

In agreement with reports on Raney-Ni [28], the results obtained in this study for hydrogen adsorbed on Raney-Co indicate the presence of different sites for hydrogen adsorption. Strongly chemisorbed hydrogen could not be removed from the surface by activation in vacuum. Hydrogen added to a pre-treated sample of Raney-Co was in parts chemisorbed and in parts physisorbed. Distinct differences observed in INS between CD_3CN and CD_3CN adsorbed on Raney-Co (compare Figs. 7 and 8) strongly suggest that the adsorbed CD_3CN was partially hydrogenated in a surface reaction. With increasing amount of co-adsorbed hydrogen, scattering contributions assigned to hydrogen increased strongly in the region around 632 and 777 cm^{-1} (hydrogen on η^3 sites with C_{3v} symmetry on the 101 plane). Scattering contributions at 504, 866, and 1020 cm^{-1} (corresponding to various vibrational modes of hydrogen on η^3 sites with C_{3v} symmetry on the 001 plane) increased to a smaller degree. Therefore, it is suggested that hydrogen adsorbed on the latter sites reacted preferably with CD_3CN. As this kind of hydrogen is more reactive, it is concluded that it is weakly chemisorbed hydrogen (see also Ref. [28]). Note that scattering contributions of intermediate species or $CD_3CH_2NH_2$ might have overlapped with bands of non-reacted hydrogen in other parts of the spectra.

4.2. Intermediate species in the co-adsorption of CD_3CN and hydrogen on Raney-Co

From the differences between the experimental spectrum of CD_3CN adsorbed on Raney-Co and the INS spectra of gas phase CD_3CN or CD_3CN adsorbed on other metals, we inferred (*vide supra*) that an intermediate species was formed by reaction of

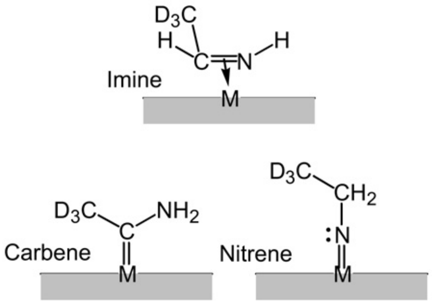

Fig. 9. Possible surface structures after reaction of CD_3CN with two hydrogen atoms [16,37].

CD_3CN with residual hydrogen on the surface. This assumption is supported by the particularly high heat of adsorption of CD_3CN at low coverage. Let us assume first that part of the adsorbed CD_3CN was fully hydrogenated to $CD_3CH_2NH_2$. The spectrum with CD_3CN adsorbed on Raney-Co has some similarities with the experimental spectrum of adsorbed $CD_3CH_2NH_2$. However, the much stronger band at 1278 cm^{-1}, and other more subtle differences, suggest that an intermediate species is formed instead, which co-exists with $CD_3CH_2NH_2$ on the surface. The most characteristic feature of the intermediate is the band at 1278 cm^{-1}. With increasing hydrogen pressure, the area of the peak at 1278 cm^{-1} decreased relative to the bands in the region above 1300 cm^{-1}, which are characteristic for $CD_3CH_2NH_2$. With increasing hydrogen concentration, the equilibrium between the intermediate and $CD_3CH_2NH_2$ is shifted to the fully hydrogenated product. Note that the position of the equilibrium implies that the partially hydrogenated surface species and adsorbed $CD_3CH_2NH_2$ are energetically comparable. In this respect, it has been shown in a molecular modelling study of amine dehydrogenation over Ni(111) that the partly dehydrogenated intermediate acimidoyl ($CH_3{-}C^*{=}NH$, where * symbolizes coordination to a metal atom) is energetically lower than adsorbed ethylamine [42].

In principle, three distinct surface structures may be possible after reaction of CD_3CN with two hydrogen atoms: (i) one hydrogen atom each attached to carbon and nitrogen forming an imine, (ii) both hydrogen atoms attached to nitrogen forming a carbene, and (iii) both hydrogen atoms attached to carbon forming a nitrene (Fig. 9). In contrast, no plausible structure for a stable intermediate can be suggested for reaction of CD_3CN with one or three hydrogen atoms.

For comparison, INS spectra of imine were calculated by DFT (Fig. 7) and the contributions of CH and NH vibrational modes distinguished by selective exchange of H atoms at the CN double bond by D atoms. The NH deformation of $CD_3CD{=}NH$ was calculated to be a low intensity band at 1348 cm^{-1}. The CH deformation of $CD_3CH{=}ND$ resulted in a band with even lower intensity at 1412 cm^{-1}. In none of the simulated spectra of the pure components, the intense band at 1278 cm^{-1} observed for the intermediate species was identified. Therefore, INS spectra of the intermediate species bound to a $Co(CO)_3$ fragment were simulated (Fig. 10). Similar to the INS spectra of the intermediate species two intensive bands at 1100 and 1225 cm^{-1} were observed for the nitrene intermediate, while the carbene intermediate did not show any characteristic bands in this region. The lower frequency might result from the quite different electronic environment of the nitrene on a $Co(CO)_3$ fragment and metallic Raney Co. Better agreement was observed for the bands of the intermediate at 1278 cm^{-1} and for adsorbed $CD_3CH_2NH_2$ at 1293 cm^{-1}, which allows the assignment of this band to a CH_2 twisting mode. Among the potential reaction intermediates, only nitrene can have CH_2 vibrational modes. The NH_2 wagging mode, which was observed for $CD_3CH_2NH_2$ as well-resolved band at 891 cm^{-1} was not observed, indicating that NH_2 groups were either not present on the surface or occurred only in very low concentrations.

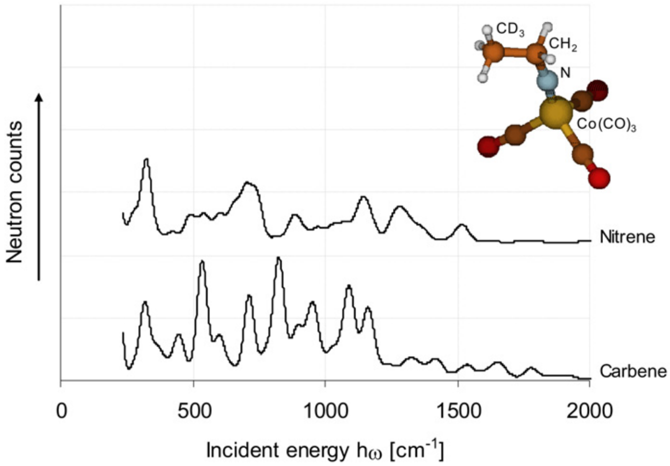

Fig. 10. Simulated INS spectra of the nitrene and carbene complexes $[Co(NCH_2CD_3)(CO)_3]$ and $[Co(C(NH_2)CD_3)(CO)_3]$, respectively. The nitrene complex is shown in the insert.

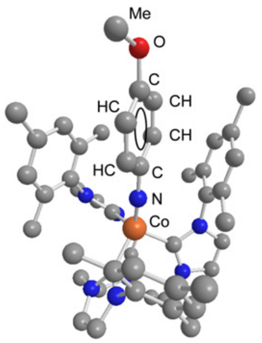

Fig. 11. Cobalt complex $[(TIMEN^{mes})Co(NC_6H_4OMe)]BPh_4$ with nitrene functionality [44], where $TIMEN^{mes}$ is a tridentate carbene ligand.

The higher intensity of the CH_2 twisting mode in nitrene relative to the CH_2 wagging and deformation modes with bands at 1359 cm^{-1} and 1455 cm^{-1}, respectively, in $CD_3CH_2NH_2$ can be explained tentatively by the different adsorption mode of the respective molecules. Note that $CD_3CH_2NH_2$ is bound *via* a M–N σ-bond, while nitrene forms a M–N double bond with the surface Co atoms. The CH_2 twisting mode leads to torsional movement of the MN bond resulting in little change in the orbital overlap of nitrogen and the metal atom. Hence, the difference between the two bonding modes should be small. The CH_2 wagging mode causes a stretch of the C–M bond, in which the change of the orbital overlap is considerably higher. As the overlap can take place more readily in an σ-bond, the CH_2 wagging may have higher intensity with $CD_3CH_2NH_2$.

Last, but not least, a search of the Cambridge Crystallographic Database provided several stable cobalt nitrene, but no carbene complexes (Fig. 11) [43,44]. This suggests that nitrenes are relatively stable and might also prevail in the hydrogenation over Raney-Co catalysts [16]. Nitrenes have also been reported in surface studies on a Ni/C catalyst [45] and suggested to be the most stable intermediates in the hydrogenation of acetonitrile over Ni surfaces [3].

5. Conclusions

Experimental and calculated INS spectra were combined with spectroscopic data from literature to investigate the formation of partly hydrogenated surface species during the hydrogenation of

CD_3CN on Raney-Co. Preliminary experiments showed that very little H/D exchange occurred. The hydrogenation proceeded with high selectivity (>90%) to $CD_3CH_2NH_2$. The only side product was the secondary amine $(CD_3CH_2)_2NH$, which resulted from hydrogenation of the reaction intermediate *N*-ethylidene-ethylamine. Concerning the Raney-Co catalyst, three adsorption sites for hydrogen were identified (strong chemisorption, chemisorption, and physisorption sites), while two different sites for adsorption of CD_3CN were identified. Hydrogen chemisorbed on η^3 sites with C_{3v} symmetry was less strongly bound than hydrogen adsorbed on other sites and, thus, most reactive. The interaction of CD_3CN with one type of sites was particularly strong, as reflected in a high heat of adsorption ($-\Delta H_{ads} = 200–215\ kJ\,mol^{-1}$). This is consistent with formation of a surface intermediate by reaction of CD_3CN with residual hydrogen. At the maximum sorption capacity for CD_3CN on the strong adsorption sites, every twelfth cobalt surface atom was occupied. This suggests that either the reaction intermediate forms a defined overlayer on the surface or the hydrogen available on the surface was consumed. The INS spectra indicated that a nitrene is formed, which was recognised by a characteristic band at $1278\ cm^{-1}$, which decreased in intensity with increasing amount of H_2 and was assigned to a CH_2 twisting mode.

Acknowledgments

The authors thank the Institut Laue-Langevin for kindly granting measuring time at the IN1-BeF spectrometer to record the INS spectra. In particular, Dr. Alexander Ivanov and Pierre Palleau are thanked for their assistance during the INS experiments. W.R. Grace & Co is thanked for the donation of the Raney-Co 2700 sample. Experimental support of Xaver Hecht and Andreas Suppan is acknowledged. Klaus Ruhland and Georgeta Krutsch from the Chair of Inorganic Chemistry are acknowledged for performing the NMR measurements.

References

[1] K. Weissermel, H.J. Arpe, Industrial Organic Chemistry, third ed., Wiley–VCH, Weinheim, 1997.
[2] J. von Braun, G. Blessing, F. Zobel, Ges. Ber. Deut. Chem. 56 (1923) 1988–2001.
[3] B. Bigot, F. Delbecq, A. Milet, V.H. Peuch, J. Catal. 159 (2) (1996) 383–393.
[4] B. Bigot, F. Delbecq, V.H. Peuch, Langmuir 11 (10) (1995) 3828–3844.
[5] M.S. Wainwright, in: G. Ertl, H. Knözinger, J. Weitkamp (Eds.), Preparation of Solid Catalysts, Wiley–VCH, Weinheim, 1999, pp. 28–43.
[6] J. Volf, J. Pasek, Stud. Surf. Sci. Catal. 27 (1986) 105–144.
[7] A. Chojecki, H. Jobic, A. Jentys, T.E. Müller, A. Lercher, J. Catal. Lett. 97 (3–4) (2004) 155–162.
[8] A. Chojecki, Selective Hydrogenation of Butyronitrile over Raney-Metals, TU München, Dissertation 2004, 116 pp.
[9] P. Schärringer, T.E. Müller, W. Kaltner, A. Lercher, J. Ind. Eng. Chem. Res. 44 (25) (2005) 9770–9775.
[10] Y.Y. Huang, W.M.H. Sachtler, Appl. Catal. A Gen. 182 (2) (1999) 365–378.
[11] Y.Y. Huang, W.M.H. Sachtler, J. Catal. 188 (1) (1999) 215–225.
[12] B. Coq, D. Tichit, S. Ribet, J. Catal. 189 (1) (2000) 117–128.
[13] C. DeBellefon, P. Fouilloux, Catal. Rev. Sci. Eng. 36 (3) (1994) 459–506.
[14] I. Ortiz-Hernandez, C.T. Williams, Langmuir 23 (6) (2007) 3172–3178.
[15] Y.Y. Huang, W.M.H. Sachtler, J. Catal. 190 (1) (2000) 69–74.
[16] Y.-Y. Huang, W.M.H. Sachtler, Stud. Surf. Sci. Catal. A 130 (2000) 527–532.
[17] R. Schenkel, A. Jentys, S.F. Parker, J.A. Lercher, J. Phys. Chem. B 108 (39) (2004) 15013–15026.
[18] S.F. Parker, N.A. Marsh, L.M. Camus, M.K. Whittlesey, U.A. Jayasooriya, G.J. Kearley, J. Phys. Chem. A 106 (24) (2002) 5797–5802.
[19] P.C.H. Mitchell, S.F. Parker, A.J. Ramirez-Cuesta, J. Tomkinson, Vibrational Spectroscopy with Neutrons: With Applications in Chemistry, Materials Science and Catalysis, World Scientific, London, 2005.
[20] S.F. Parker, J.W. Taylor, P. Albers, M. Lopez, G. Sextl, D. Lennon, A.R. McInroy, I.W. Sutherland, Vib. Spectrosc. 35 (1–2) (2004) 179–182.
[21] S. Vasudevan, J.M. Thomas, C.J. Wright, C. Sampson, Soc. J. Chem. Chem. Commun. 7 (1982) 418–419.
[22] R. Schenkel, A. Jentys, S.F. Parker, J.A. Lercher, J. Phys. Chem. B 108 (23) (2004) 7902–7910.
[23] H. Jobic, A. Renouprez, J. Chem. Soc. Faraday Trans. I 80 (1984) 1991–1997.
[24] F. Hochard, H. Jobic, G. Clugnet, A. Renouprez, J. Tomkinson, Catal. Lett. 21 (3–4) (1993) 381–389.
[25] F. Hochard, H. Jobic, J. Massardier, A.J. Renouprez, J. Mol. Catal. A Chem. 95 (2) (1995) 165–172.
[26] M. Hesse, H. Meier, B. Zeeh, Spektroskopische Methoden in der organischen Chemie, third ed., Georg Thieme Verlag, Stuttgart, 1987, p. 318.
[27] E. Pretsch, T. Clerc, J. Seibl, S. Wilhelm, Tabellen zur Strukturaufklärung organischer Verbindungen mit spektroskopischen Methoden, in: W. Fresenius (Ed.), Anleitungen für die chemische Laboratoriumspraxis, vol. 15, third ed., Springer-Verlag, Berlin, 1986.
[28] http://www.ill.fr/YellowBook/IN1.
[29] M.J. Frisch, G.W. Trucks, H.B. Schlegel, G.E. Scuseria, M.A. Robb, J.R. Cheeseman, J.A. Montgomery, Jr., T. Vreven, K.N. Kudin, J.C. Burant, J.M. Millam, S.S. Iyengar, J. Tomasi, V. Barone, B. Mennucci, M. Cossi, G. Scalmani, N. Rega, G.A. Petersson, H. Nakatsuji, M. Hada, M. Ehara, K. Toyota, R. Fukuda, J. Hasegawa, M. Ishida, T. Nakajima, Y. Honda, O. Kitao, H. Nakai, M. Klene, X. Li, J.E. Knox, H. Hratchian, J.B. Cross, C. Adamo, J. Jaramillo, R. Gomperts, R.E. Stratmann, O. Yazyev, A.J. Austin, R. Cammi, C. Pomelli, J.W. Ochterski, P.Y. Ayala, K. Morokuma, G.A. Voth, P. Salvador, J.J. Dannenberg, V.G. Zakrzewski, S. Dapprich, A.D. Daniels, M.C. Strain, O. Farkas, D.K. Malick, A.D. Rabuck, K. Raghavachari, J.B. Foresman, J.V. Ortiz, Q. Cui, A.G. Baboul, S. Clifford, J. Cioslowski, B.B. Stefanov, G. Liu, A. Liashenko, P. Piskorz, I. Komaromi, R.L. Martin, D.J. Fox, T. Keith, M.A. Al-Laham, C.Y. Peng, A. Nanayakkara, M. Challacombe, P.M.W. Gill, B. Johnson, W. Chen, M.W. Wong, C. Gonzalez, J.A. Pople, Gaussian 03, Revision B.04, Gaussian, Inc., Pittsburgh PA, 2003.
[30] D. Champion, J. Tomkinson, G. Kearley, Appl. Phys. A Math. Sci. Proc. 74 (2002) S1302–S1304.
[31] A.J. Ramirez-Cuesta, Comp. Phys. Commun. 157 (3) (2004) 226–238.
[32] A. Chojecki, M. Veprek-Heijman, T.E. Müller, P. Schärringer, S. Veprek, J.A. Lercher, J. Catal. 245 (2007) 237–248.
[33] A. Jentys, R.R. Mukti, H. Tanaka, J.A. Lercher, Microporous Mesoporous Mater. 90 (1–3) (2006) 284–292.
[34] C.M. Friend, E.L. Muetterties, J.L. Gland, J. Phys. Chem. 85 (22) (1981) 3256–3262.
[35] D.E. Gardin, G.A. Somorjai, J. Phys. Chem. 96 (23) (1992) 9424–9431.
[36] B.A. Sexton, N.R. Avery, Surf. Sci. 129 (1) (1983) 21–36.
[37] J.E.D. Davies, J. Mol. Struct. 9 (4) (1971) 483.
[38] J.L. Gland, G.B. Fisher, G.E. Mitchell, Chem. Phys. Lett. 119 (1) (1985) 89–92.
[39] Y. Hamada, K. Hashiguchi, A.Y. Hirakawa, M. Tsuboi, M. Nakata, M. Tasumi, S. Kato, K. Morokuma, J. Mol. Spectrosc. 102 (1) (1983) 123–147.
[40] H. Wolff, H. Ludwig, J. Chem. Phys. 56 (11) (1972) 5278.
[41] H. Wolff, H. Ludwig, Ber. Bunsen-Ges. Phys. Chem. 71 (8) (1967) 911.
[42] P.D. Ditlevsen, D.E. Gardin, M.A. Vanhove, G.A. Somorjai, Langmuir 9 (6) (1993) 1500–1503.
[43] D.T. Shay, G.P.A. Yap, L.N. Zakharov, A.L. Rheingold, K.H. Theopold, Angew. Chem. Int. Ed. 44 (10) (2005) 1508–1510.
[44] X. Hu, K. Meyer, J. Am. Chem. Soc. 126 (50) (2004) 16322–16323.
[45] H. Bock, O. Breuer, Angew. Chem. Int. Ed. Engl. 26 (5) (1987) 461–462.